P1.2 SENSITIVITY OF WRF MODEL FORECASTS TO DIFFERENT PHYSICAL PARAMETERIZATIONS IN THE BEAUFORT SEA REGION

Jeremy R. Krieger *, Jing Zhang
Arctic Region Supercomputing Center, University of Alaska Fairbanks

David E. Atkinson, Xiangdong Zhang
International Arctic Research Center, University of Alaska Fairbanks

Martha D. Shulski
Geophysical Institute, University of Alaska Fairbanks

1. INTRODUCTION

The Weather Research and Forecasting (WRF) model has been applied to the Beaufort Sea region to investigate the mesoscale features of the Beaufort Sea surface winds. One of the foremost challenges in establishing a mesoscale model for use in a particular region is the determination of the most appropriate model configuration. Different regions experience varied conditions and present unique problems, and the optimal setup for one area may therefore generate poorer results in another. One of the most important elements in configuring a model is the selection of the physical parameterizations to be used. While current models provide a large pool of options from which to choose schemes governing several different types of model physics, this diversity presents its own problems for the modeler, as identifying the best physics package becomes highly complex. Aside from the existence of a large array of available options, the best combination for one region is not necessarily applicable to another.

The Beaufort Sea region, including the North Slope of Alaska, is a particularly unique area. Though previous studies have attempted to determine the best physics options to use in polar regions (Hines and Bromwich 2008), their conclusions are not necessarily fully applicable to this region, with its combination of complex geographical features, including a sea covered by seasonal sea ice with a coast that borders a rugged mountain range. We have conducted a series of month-long sensitivity simulations with the WRF model to attempt to identify the best-performing physics package for this region. In the simulations, all available physics options have been tested and the results verified against observations from not only land-based stations, but also from the QuikSCAT SeaWinds instrument, which provides high-resolution surface wind data over the open ocean. Through this statistical analysis, we aim to ascertain the most suitable combination of physical schemes applicable to the Beaufort Sea region as a whole, including both land and ocean areas, with a special emphasis given to evaluating the simulation of surface winds over the sea.

* *Corresponding author address:* Jeremy Krieger, Arctic Region Supercomputing Center, University of Alaska Fairbanks, Fairbanks, AK 99775; e-mail: krieger@arsc.edu

2. MODEL AND CONFIGURATION

The model used to conduct the simulations in this study is the Advanced Research WRF (ARW) v3.0 (Skamarock and Klemp 2008), a widely used community mesoscale model developed by the National Center for Atmospheric Research (NCAR). It represents the current state-of-the-science in mesoscale model development, and was established as a successor to the long-standing Penn State/NCAR Fifth-Generation Mesoscale Model (MM5), sharing much of the same dynamics and model physics. Though WRF is a relatively young model, a variety of studies have been carried out investigating the performance of the various available physical parameterizations in accurately simulating weather conditions in varied geographic regions (e.g. Jankov et al. 2005; Gallus and Bresch 2006; Jankov et al. 2007). However, very few have tested these schemes in arctic conditions, except for the efforts related to the development of the Polar WRF (Hines and Bromwich 2008). However, this work is based on an older version of the WRF model (v2.1) than the one currently available. Since v2.1, many modifications, bug fixes, and more advanced parameterizations have been added to the model. Some of these are of particular import to polar regions and for use in high resolution simulations, such as the Morrison et al. 2-moment (Morrison et al. 2008) and Goddard (Tao and Simpson 1993) microphysics schemes. There also exists new land-surface model (LSM) (Xiu and Pleim 2001) and planetary boundary layer (PBL) schemes (Pleim 2007), which could have significant impacts on the simulation of near-surface conditions. All of these factors necessitate further testing of WRF v3.0 for our particular region of interest.

Complex geographic features make the accurate modeling of high-resolution atmospheric conditions in the Beaufort Sea region rather difficult, and further require a model to be sufficiently tested before being used in the area. In order to accomplish this, we established the modeling domain as shown in Figure 1, encompassing the entire North Slope and Brooks Range, as well as the Chukchi and Beaufort Seas and portions of the Canadian Yukon and the eastern tip of Russia. The domain has dimensions of 235 x 136 points with a grid spacing of 10 km and 43 vertical levels.

The oceanic portion of the domain experiences high variability throughout the year in its sea ice coverage,

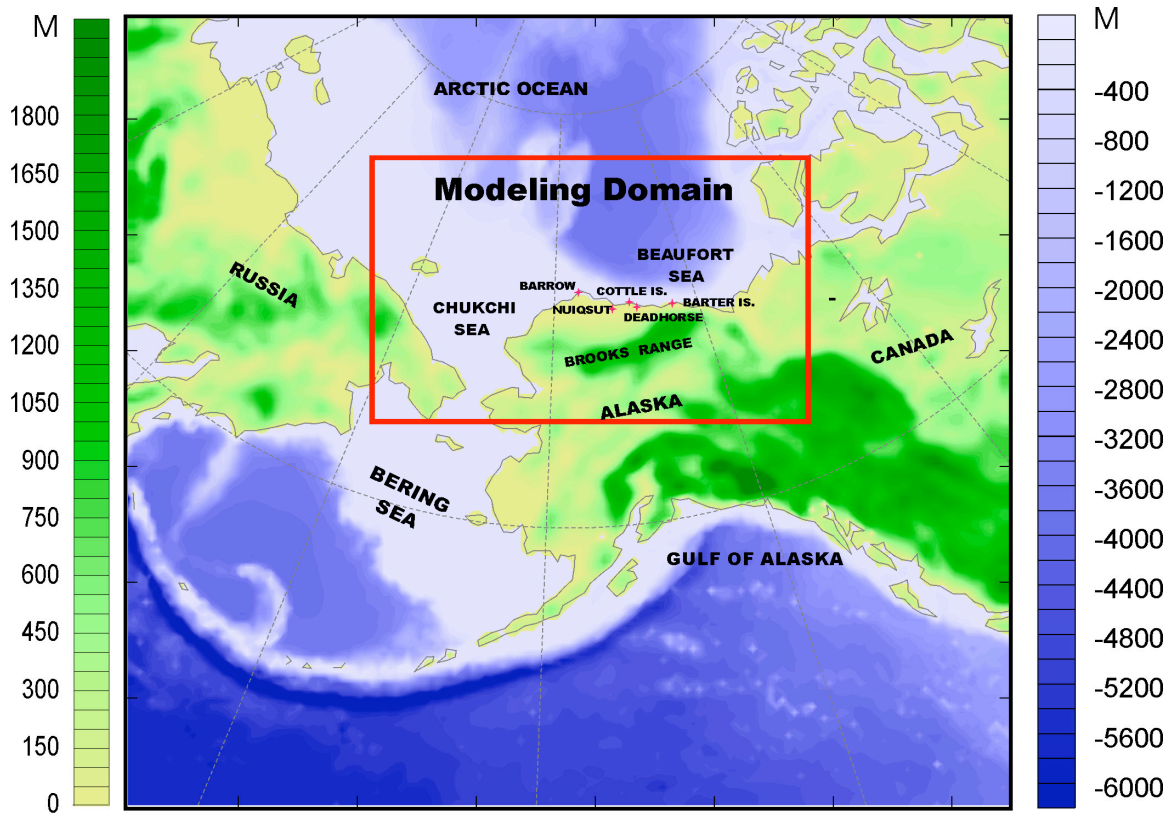

Figure 1. WRF modeling domain (red box) encompassing the Beaufort and Chukchi Seas, the North Slope of Alaska, and the Brooks Range. Some stations used for verification are indicated with red dots.

and the land portion similarly varies in its snow coverage, both of which are important to the thermal contrast that exists between land and ocean and that has a significant role in driving the near-surface circulation patterns. As such, to properly test the model's performance it is essential to select a representative simulation time period that contains both ice-free and ice-covered ocean, as well as bare and snow-covered land, and includes the transition period between the two states. We chose the month of September 2004 as our test period. In addition to representing the time of year when the transition from snow-free to snow-covered land takes place, this is also when the ice-free area off of the Beaufort Sea coast is at its maximum (while still containing portions of ice-covered ocean). This fact has the added benefit of allowing us to use a large amount of ocean-based observations from the QuikSCAT satellite to validate the model. In conducting the simulations, we subdivided the month into eight 4.5-day periods that were run independently, initialized at 12 UTC of each fourth day, with the first 12 hours of each simulation used as spinup and not used in the validation. Thus, in stitching together the final four days of each simulation, we were able to create hourly time series extending from 00 UTC Sep 02 – 00 UTC Oct 04, which were then used for verification.

In order to perform as complete a test as possible of the available physical parameterizations, we began with an experiment that utilized WSM 6-class microphysics, CAM longwave and shortwave radiation (Collins et al. 2004), Kain-Fritsch cumulus (Kain 2004), YSU PBL (Hong et al. 2006), and the NOAH LSM (Chen and Dudhia 2001), which we then designated as the control run (CTRL). From this, we varied each of the physics types in turn, for each type cycling through the available options and producing a time series for each option. We tested a total of 6 cumulus, 6 microphysics, 2 longwave (LW), 3 shortwave (SW), 4 planetary boundary layer (PBL), and 3 land-surface options, as summarized in Table 1. In addition, we performed one combination test using the Pleim-Xiu LSM and ACM2 PBL, two schemes that were developed in conjunction with one another by the same research team, as well as the six combinations of longwave and shortwave radiation. This resulted in a total of 21 month-long time series that were then verified against observations.

3. VERIFICATION DATA

Hourly in situ observations from 21 surface stations throughout the North Slope, both coastal and inland, were used to verify the model output. In addition to the in situ data, model data was also verified against observations from the SeaWinds instrument onboard NASA's Quick Scatterometer (QuikSCAT) satellite. This dataset consists of measurements of surface (10-m) wind speed and direction, which are measured at a

CTRL	Control (Kain-Fritsch cumulus, WSM 6-class microphysics, CAM LW + CAM SW, NOAH LSM, YSU PBL)
Cumulus	
NOCU	No cumulus scheme
BMJ	Betts-Miller-Janjic (Janjic 1994)
GD	Grell-Devenyi (Grell and Devenyi 2002)
GREL	Grell-3
KFO	Old Kain-Fritsch (Kain and Fritsch 1993)
Microphysics	
MORR	Morisson 2-moment
LIN	Purdue Lin (Chen and Sun 2002)
ETA	Eta
GODD	Goddard
THOM	Thompson (Thompson et al. 2004)
Radiation	
LW1SW1	Rapid Radiative Transfer Model (RRTM) LW (Mlawer et al. 1997) + Dudhia SW (Dudhia 1989)
LW1SW2	RRTM LW + Goddard SW (Chou and Suarez 1994)
LW1SW3	RRTM LW + CAM SW
LW3SW1	CAM LW + Dudhia SW
LW3SW2	CAM LW + Goddard SW
LSM	
RUC	Rapid Update Cycle model (Smirnova et al. 2000)
PX	Pleim-Xiu
PBL	
MYJ	Mellor-Yamada-Janjic (Janjic 2002)
ACM2	Asymmetrical Convective Model 2
MRF	Medium Range Forecast model (Hong and Pan 1996)
Combination	
PX2	PX + ACM2

Table 1. Simulation Experiments – Aside from the indicated scheme(s), all others are as in the control.

spacing of ~12 km and are available over the open ocean, to within ~30 km of the coastline. As no permanent buoys are located in the Beaufort Sea due to the movement of sea ice, and as such very little oceanic in situ data is available in this region, QuikSCAT data is an invaluable resource for providing surface wind observations over the Beaufort Sea. For this study, QuikSCAT observations were grouped into one-hour windows and used to verify the model output at the top of each hour.

4. RESULTS

Modeled surface (2-m) temperature and dew point, (10-m) wind speed and direction, and sea level pressure were verified against the station observations and QuikSCAT data described in Section 3. For each variable, the model data were interpolated to the station/satellite location and the root-mean-square error (RMSE), mean bias, and correlation coefficient were calculated over the entire simulation period.

4.1. In situ verification

Figure 2 shows the results of the cumulus parameterization sensitivity tests concerning surface wind speed and direction, with experiment identifiers as given in Table 1. From these plots, it is clear that the control run (Kain-Fritsch) outperformed all of the other available options. Not only did it produce the minimum RMSE for both speed and direction, but it generated the smallest absolute bias (closest to zero) and had the highest correlation coefficient for speed as well. As would be expected for an arctic region, where convective activity is not a significant factor, even in the summer, the differences in the performance of the various schemes is not altogether great, especially compared to differences seen with other physics types. Despite this, however, the Kain-Fritsch scheme did prove itself to be consistently better than the others over the course of the month. One other thing to note from these results is that the worst performing option is running the model without any cumulus scheme at all. Even with a relatively high grid resolution and in a rather non-convective environment, the use of any cumulus parameterization appears to be warranted.

A similar comparison is shown in Figure 3, this time for the microphysics sensitivity tests. As for the convective schemes, a clear favorite is demonstrated as the Lin scheme outperformed all the others in every measure of wind speed and direction. It produced the lowest RMSE, minimum absolute bias, and maximum correlation. Also of note here is the relatively poor performance of the Thompson and Morrison schemes, which are the most advanced and complex of the group. The results of Morrison are especially surprising given that it is a 2-moment scheme, which would normally be expected to produce superior results in polar regions where the accurate simulation of mixed-phase clouds is especially important. However, it should be mentioned that subsequent to these simulations the WRF development group issued a bug fix for this scheme; if these simulations were rerun with the bug fix incorporated, it is possible that the results would be improved to some degree.

The same comparison for the various radiation option combinations is given in Figure 4. Unlike the case with the cumulus and microphysics tests, none of the schemes produced superior results over all four measures. The minimum wind speed RMSE is produced by RRTM LW / CAM SW (LW1SW3); however, it also generated the second largest direction RMSE. In contrast, CAM LW / Goddard SW (LW3SW2) performed best when looking at direction RMSE, but also resulted in the second highest error in speed and a relatively large absolute bias. Overall, the only absolutely clear result is the very poor performance of the CAM LW / Dudhia SW (LW3SW1) combination. By every measure, it performed significantly worse than all other combinations, as well as producing substantially more error-prone surface temperatures (not shown), suggesting that this combination of radiation schemes should be used only with the greatest caution.

In Figure 5, the error statistics are presented for the three land surface models currently available in WRF, plus the additional combination of the Pleim-Xiu LSM and ACM2 PBL schemes (PX2). From this, it is clear that winds are generally better simulated when the Pleim-Xiu scheme is used, whether or not the ACM2 PBL is used in conjunction. One or the other bests both NOAH (control) and RUC in every category. Surprising results are seen from the NOAH LSM, which produced relatively high errors, a large negative bias, and a small correlation. NOAH has generally been favored by the research community, and, though its surface temperature results were superior to the others (not shown), this serves to emphasize the need for rigorous testing of the various parameterizations in the model. As our own research needs are focused on the simulation of surface winds, these surprising results have great significance, and point out that researchers should not always take the superiority of a particular scheme for granted.

Finally, Figure 6 shows the comparison of the results of the PBL sensitivity tests. The choice of a PBL scheme is arguably the most important of the model physics types when looking at near-surface atmospheric parameters, as it handles the highly complex interactions and fluxes between the surface layer and free atmosphere, and is used to calculate the 2-m temperature and dew point and 10-m winds which are ultimately used for verification of the modeling results. This figure further highlights the strong performance of the Pleim-Xiu / ACM2 combination (PX2), as it outperformed all other PBL schemes in every measure. It is interesting to note, however, that by itself the ACM2 PBL did not generate nearly as positive results (aside from the direction RMSE). This is significant, and highlights the need to test various combinations of the available schemes, that simply varying one at a time may not properly capture the (potentially beneficial) interactions that can possibly result between different parameterizations.

4.2. QuikSCAT verification

Though, given their nature, satellite-based measurements are not as robust as in situ observations, they nevertheless provide a valuable resource for providing coverage over data sparse regions. Our model domain is one such region, as nearly half of it is covered by ocean that contains no permanent buoys. Since our efforts are ultimately directed at simulating surface winds over the Beaufort and Chukchi Seas, it is therefore of critical importance to attempt to verify modeled data over the oceanic areas as well. QuikSCAT observations allow us to do that.

Similar comparisons as were made for the station observations are shown in Figure 7. For brevity, only RMSE for speed and direction is shown. As for the case with station verification, the Kain-Fritsch cumulus, Pleim-Xiu LSM, and Pleim-Xu / ACM2 PBL combination produced the most accurate simulations of surface winds in their respective categories. A notable difference arises, however, when looking at microphysics. In contrast to the stations, for which Lin produced better results, in this case Eta outperformed the rest. Also, in the radiation comparison, the control (CAM LW & SW) and CAM LW / Goddard SW were noticeably better than the others. This contrasts with the land observations, for which there were no clear favorites.

While it is encouraging that the same convective scheme and LSM and PBL combination generated the most accurate results in both the in situ and QuikSCAT comparisons, the discrepancy in the identity of the best microphysics scheme between land and ocean points suggests that more work is needed in order to positively identify which is the best overall to use. Additional testing for different times of year needs to be conducted in order to better identify which of the microphysics and radiation schemes are consistently better than the others for this particular region.

5. SUMMARY AND CONCLUSIONS

A sensitivity analysis was conducted using the WRF model (v3.0) in order to ascertain which of the available physics options will generate the most accurate results for the Beaufort Sea region, focusing on the model's capability in simulating surface winds. A series of sensitivity runs were conducted over the month of September 2004 and the results were verified against both in situ station observations and QuikSCAT ocean-surface wind data.

It was found that the Kain-Fritsch cumulus, Lin microphysics, Pleim-Xu land surface, and PX / ACM2 PBL combination clearly generated the most accurate surface wind results as compared to station observations, while the results of the various radiation schemes were more mixed. Compared to QuikSCAT data, the Kain-Fritsch, Pleim-Xu, and ACM2 PBL again performed well, whereas the Eta microphysics proved to be superior and there was more differentiation among the radiation parameterizations than was seen for the land observations.

These results, particularly the performance of the PX / ACM2 combination, suggest that it is important to consider the interactions between various model physical parameterizations, and that it is not sufficient to vary one at a time relative to a control run in order to determine the best overall combination. Rather, it is necessary to test many different configurations in order to determine the optimal setup for any particular region. As we move forward, we aim to use the best-performing individual schemes as found in this study as the basis for a new round of sensitivity testing, in which additional sets of permutations will be examined. The disparity in the best-performing microphysics parameterizations between land and ocean points also highlights the need to evaluate such tests over a wide domain and in varying climatological conditions.

It should be stressed that the results presented herein are of surface winds alone, and that when looking at other parameters such as surface temperature and dew point the relative rankings of the various schemes can be changed. One that

underperforms in the simulation of wind (such as NOAH) can in fact produce superior outcomes for other, thermodynamic variables. As our project is concerned primarily with the accurate depiction of surface winds, how well the model simulates these is naturally our top concern, and the results and analysis given in this paper reflect that. The relative success of a given parameterization in simulating surface winds can and should not be interpreted as applying to any other parameters.

Acknowledgements: This work was supported by DOI/MMS under contract 0106CT39787 and the Arctic Region Supercomputing Center at the University of Alaska Fairbanks.

6. REFERENCES

Chen, F. and J. Dudhia, 2001: Coupling an advanced land-surface hydrology model with the PSU/NCAR MM5 modeling system. Part I: Model description and implementation. *Mon. Wea. Rev.*, 129, 569–585.

Chen, S.-H., and W.-Y. Sun, 2002: A one-dimensional time dependent cloud model. *J. Meteor. Soc. Japan*, 80, 99–118.

Chou M.-D. and M. J. Suarez, 1994: An efficient thermal infrared radiation parameterization for use in general circulation models. NASA Tech. Memo. 104606, 3, 85 pp.

Collins, W.D. et al., 2004: Description of the NCAR Community Atmosphere Model (CAM3.0), NCAR Technical Note, NCAR/TN-464+STR, 226 pp.

Dudhia, J., 1989: Numerical study of convection observed during the winter monsoon experiment using a mesoscale two-dimensional model, *J. Atmos. Sci.*, 46, 3077–3107.

Gallus, W. A. and J. F. Bresch, 2006: Comparison of impacts of WRF dynamic core, physics package, and initial conditions on warm season rainfall forecasts. *Mon. Wea. Rev.*, 134, 2632–2641.

Grell, G. A., and D. Devenyi, 2002: A generalized approach to parameterizing convection combining ensemble and data assimilation techniques. *Geophys. Res. Lett.*, 29(14), Article 1693.

Hines, K. M. and D. H. Bromwich, 2008: Development and testing of Polar Weather Research and Forecasting (WRF) Model. Part I: Greenland ice sheet meteorology. *Mon. Wea. Rev.*, 136, 1971–1989.

Hong, S.-Y., Y. Noh, and J. Dudhia, 2006: A new vertical diffusion package with an explicit treatment of entrainment processes. *Mon. Wea. Rev.*, 134, 2318–2341.

Hong, S.-Y., and H.-L. Pan, 1996: Nonlocal boundary layer vertical diffusion in a medium-range forecast model. *Mon. Wea. Rev.*, 124, 2322–2339.

Janjic, Z. I., 1994: The step-mountain eta coordinate model: Further developments of the convection, viscous sublayer and turbulence closure schemes. *Mon. Wea. Rev.*, 122, 927–945.

Janjic, Z. I., 2002: Nonsingular Implementation of the Mellor–Yamada Level 2.5 Scheme in the NCEP Meso model. NCEP Office Note, No. 437, 61 pp.

Jankov, I., W. A. Gallus, M. Segal, B. Shaw, and S. E. Koch, 2005: The impact of different WRF model physical parameterizations and their interactions on warm season MCS rainfall. *Wea. and Forecasting*, 20, 1048–1060.

Jankov, I., P. J. Schultz, C. J. Anderson, and S. E. Koch, 2007: The impact of different physical parameterizations and their interactions on cold season QPF in the American River basin. *J. Hydromet.*, 8, 1141–1151.

Kain, J. S., 2004: The Kain-Fritsch convective parameterization: An update. *J. Appl. Meteor.*, 43, 170–181.

Kain, J. S., and J. M. Fritsch, 1993: Convective parameterization for mesoscale models: The Kain-Fritcsh scheme, *The representation of cumulus convection in numerical models*, K. A. Emanuel and D.J. Raymond, Eds., Amer. Meteor. Soc., 246 pp.

Mlawer, E. J., S. J. Taubman, P. D. Brown, M. J. Iacono, and S. A. Clough, 1997: Radiative transfer for inhomogeneous atmosphere: RRTM, a validated correlated-k model for the longwave. *J. Geophys. Res.*, 102 (D14), 16663–16682.

Morrison, H., G. Thompson, and V. Tatarskii, 2008: Impact of cloud microphysics on the development and trailing stratiform precipitation in a simulated squall line: Comparison of one- and two-moment schemes. Submitted to *Mon. Wea. Rev.*

Pleim, J. E., 2007: A combined local and non-local closure model for the atmospheric boundary layer. Part I: Model description and testing. *J. Appl. Meteor. and Clim.*, 46, 1383–1395.

Skamarock, W. C. and J. B. Klemp, 2008: A time-split nonhydrostatic atmospheric model for weather research and forecasting applications. *J. Comp. Phys.*, 227, 3465–3485.

Smirnova, T. G., J. M. Brown, S. G. Benjamin, and D. Kim, 2000: Parameterization of cold-season processes in the MAPS land-surface scheme. *J. Geophys. Res.*, 105 (D3), 4077–4086.

Tao, W.-K. and J. Simpson, 1993: The Goddard cumulus ensemble model. *Terr. Atmos. Oceanic Sci.*, 4, 35–72.

Thompson, G., R. M. Rasmussen, and K. Manning, 2004: Explicit forecasts of winter precipitation using an improved bulk microphysics scheme. Part I: Description and sensitivity analysis. *Mon. Wea. Rev.*, 132, 519–542.

Xiu, A. and J. E. Pleim, 2001: Development of a land surface model. Part I: Application in a mesoscale meteorological model. *J. Appl. Meteor.*, 40, 192–209.

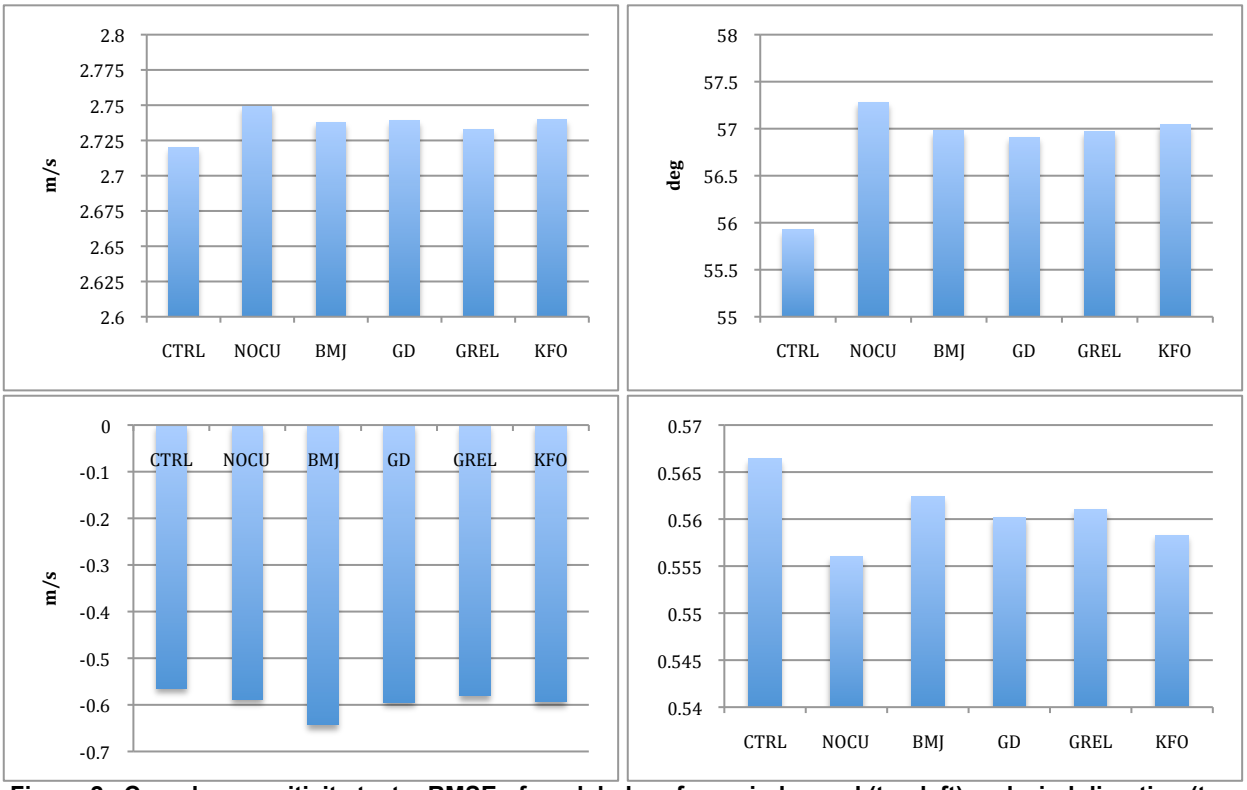

Figure 2. Cumulus sensitivity tests: RMSE of modeled surface wind speed (top left) and wind direction (top right); mean bias of wind speed (bottom left); correlation coefficient of wind speed (bottom right); as compared to stations

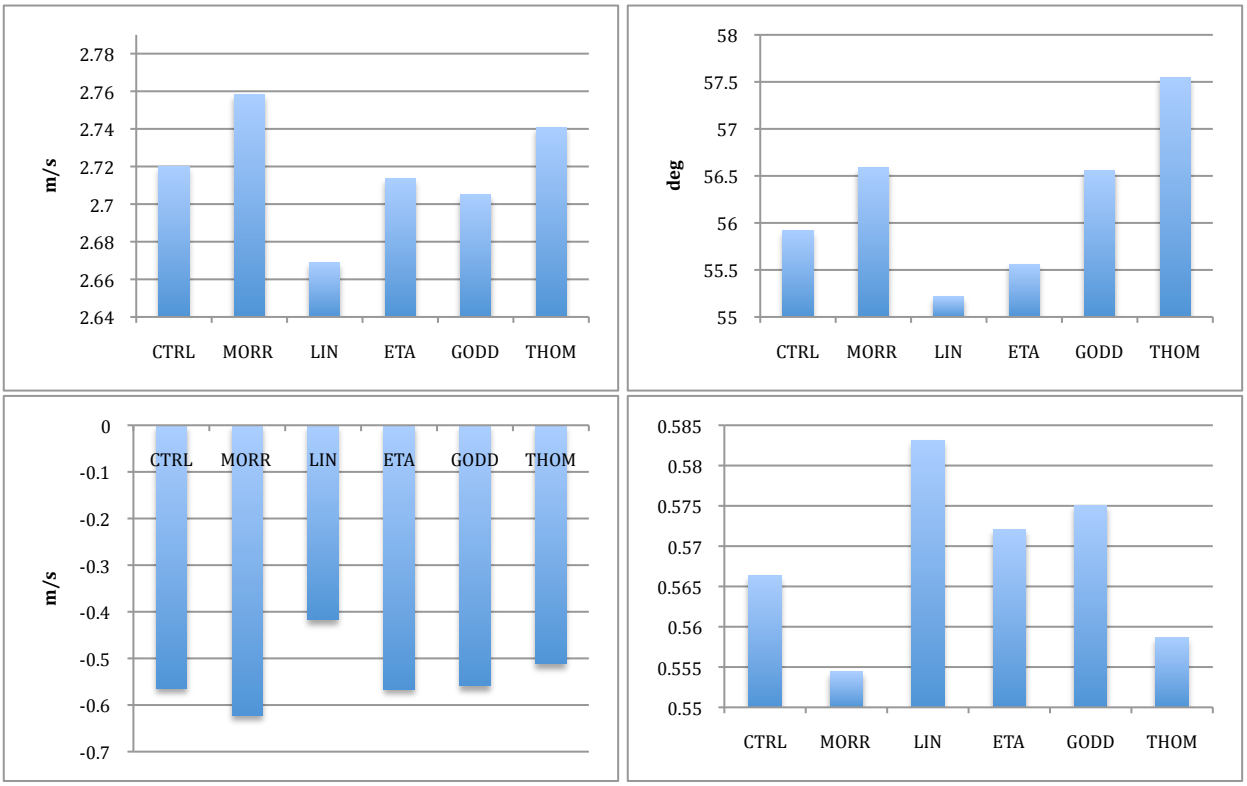

Figure 3. Same as Fig. 2 but for microphysics tests

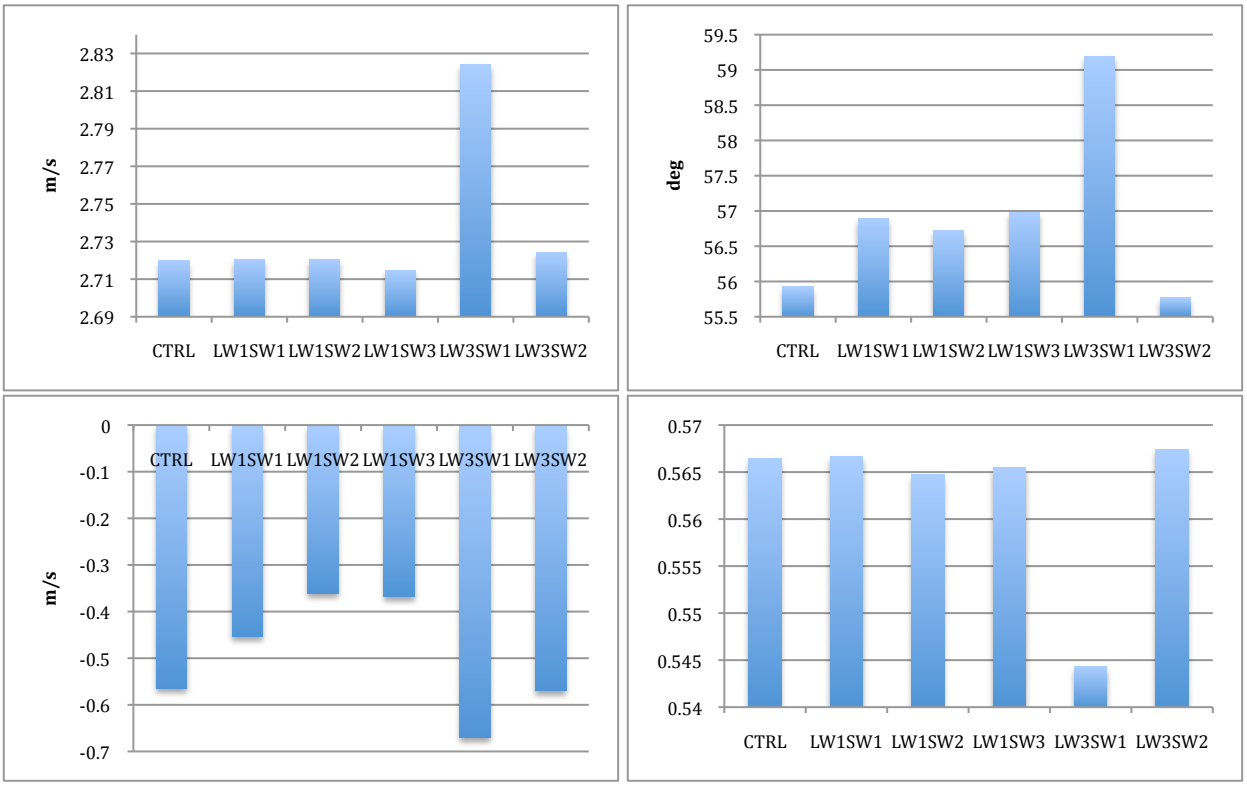

Figure 4. Same as Fig. 2 but for radiation tests

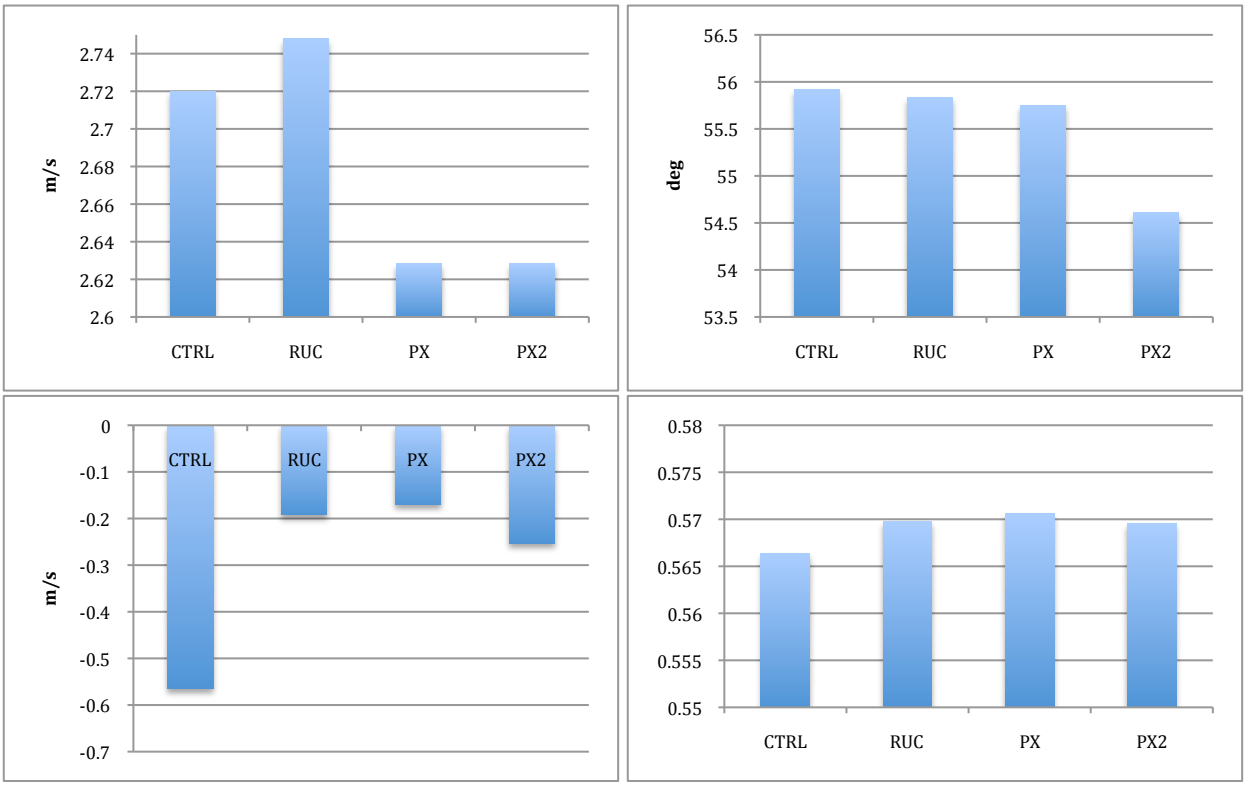

Figure 5. Same as Fig. 2 but for LSM tests

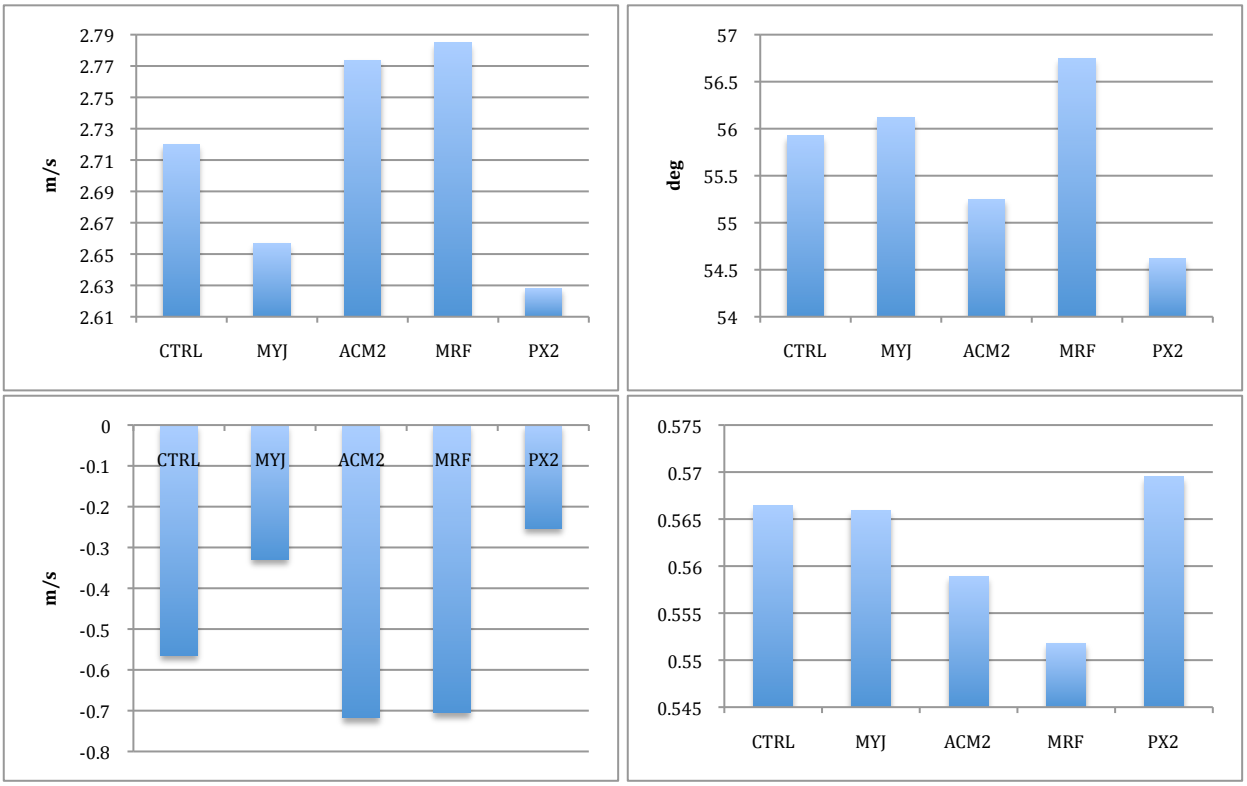

Figure 6. Same as Fig. 2 but for PBL tests

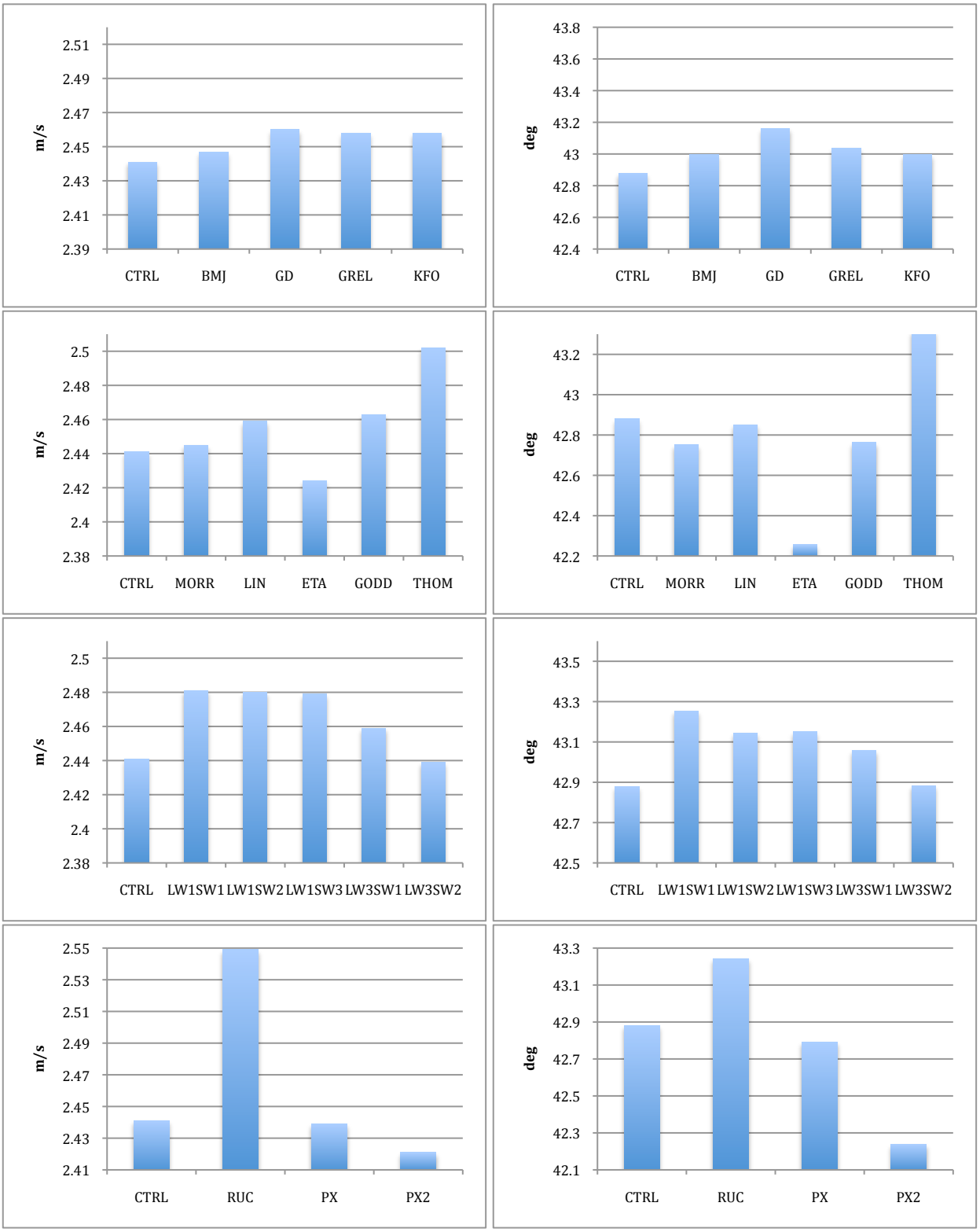

Figure 7. RMSE of wind speed (left) and direction (right) for (from top to bottom) cumulus, microphysics, radiation, and LSM tests as compared to QuikSCAT observations

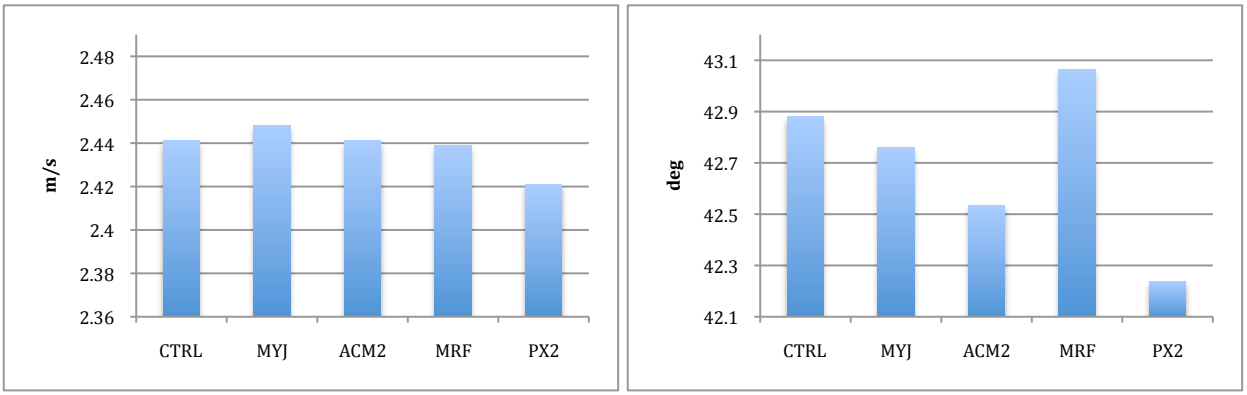

Figure 7 (cont). PBL tests